ELSEVIER

Journal of Biomechanics 40 (2007) 2467–2476

JOURNAL OF BIOMECHANICS

www.elsevier.com/locate/jbiomech
www.JBiomech.com

Experimental validation of intact and implanted distal femur finite element models

A. Completo[a], F. Fonseca[b], J.A. Simões[a,*]

[a]*Departamento de Engenharia Mecânica, Universidade de Aveiro, 3810-193 Aveiro, Portugal*
[b]*Faculdade de Ciências da Saúde, Universidade da Beira Interior, 6201-001 Covilhã, Portugal*

Accepted 10 November 2006

Abstract

Four finite element (FE) models of intact and distal femur of knee replacements were validated relative to measured bone strains. FE models of linear tetrahedrons were used. Femoral replacements with cemented stemless, cemented and noncemented femoral stems of the PFC Sigma Modular Knee System were analyzed. Bone strains were recorded at ten locations on the cortex. The magnitude of the FE bone strains corresponded to the mean measured strains, with an overall agreement of 10%. Linear regression between the FE and mean experimental strains produced slopes between 0.94 and 1.06 and R_2 values between 0.92 and 0.99. RSME values were less than 12%. The FE models were able to adequately replicate the mechanical behavior of distal femur reconstructions.

Keywords: Distal femur; Knee prosthesis; Composite femur; Finite-element analysis; Strain gauge measurements

1. Introduction

There exists much literature dealing with finite element (FE) and experimental in vitro studies for the measurement of strain on the surface of femurs and tibias. Most of the literature deals with the measurement of strain on the surface of proximal femurs to respond to a clinical need to investigate in vitro implant–bone load transfer mechanisms as well as to monitor the stress shielding effect due to implantation of hip (Huiskes et al., 1992). Much lesser FE and experimental studies are available relative to the distal femur.

Commercially available synthetic femurs have been extensively used in predicting biomechanically the performance of hip prostheses (Heiner and Brown, 2001; Cristofolini et al., 1998; Cristofolini and Viceconti, 1997; Dias Rodrigues et al., 2004; Grecula et al., 2000; Simões and Vaz, 2002; Stolk et al., 2000, 2002; Szivek and Gealer, 1991; Viceconti et al., 1998) and are used as substitutes of cadaveric specimens. Synthetic bones are useful for comparative tests (Viceconti et al., 1996). Although these synthetic bones are not able to represent the biological response of natural femurs, their geometrical and mechanical characteristics have been validated to fall within the range of those of cadaveric specimens (Cristofolini et al., 1996; Szivek and Gealer, 1991; McNamara et al., 1994). These synthetic bones also minimize interspecimen variability.

The synthetic proximal femur is very well validated, but there is a lack of investigation about the biomechanics of the distal femur. Cristofolini et al. (1998), in a different context than the one described in this paper, defined the strain pattern in the host bone following distal femoral resection and implantation of a massive prosthesis. Some studies have been performed with cadaveric femur bones and strains have been measured on the surface of the femur (Crowninshield et al., 1980; Szivek and Gealer, 1991; Young-Hoo et al., 2001). Other studies have shown the adequacy of synthetic femurs to obtain similar strain distributions as those that occur due to bending, torsion and compression loads in the human femur (Cristofolini and Viceconti, 2000; Heiner and Brown, 2001; Szivek et al., 1993). Heiner and Brown (2001) showed that the

*Corresponding author. Tel.: +351 234370830; fax: +351 234370953.
E-mail address: simoes@mec.ua.pt (J.A. Simões).

0021-9290/$ - see front matter © 2006 Elsevier Ltd. All rights reserved.
doi:10.1016/j.jbiomech.2006.11.012

repeatability of these models is superior to those obtained with cadaveric femur bones and is within the range of 0.5–7.8%. The variability between synthetic femurs is around 4.5% (Heiner and Brown, 2001).

The quality of FE models depends on several simulation factors. The models should be sufficiently refined to represent accurately the geometry and mechanical behavior of the bone structure they simulate (Huiskes and Chao, 1983; Verma and Melosh, 1987). The results are mesh sensitive and ideally a convergence test should be performed to test the model accuracy.

In the current study, FE models of implanted distal femur with a range of knee prostheses used in total knee replacement (standard nonstemmed, short cemented stem, and long noncemented stem) have been validated according to experimental cortex bone strains. These reconstructions were evaluated to investigate a full range of possible load transfer conditions that may be applicable clinically. This was done to test the robustness of the modeling procedure and the FE models developed can be used for pre-clinical testing of femoral knee replacements like load transfer conditions and long-term failure scenarios. This knowledge provides a good basis for further development of a standardized FE pre-clinical test for femoral knee replacements.

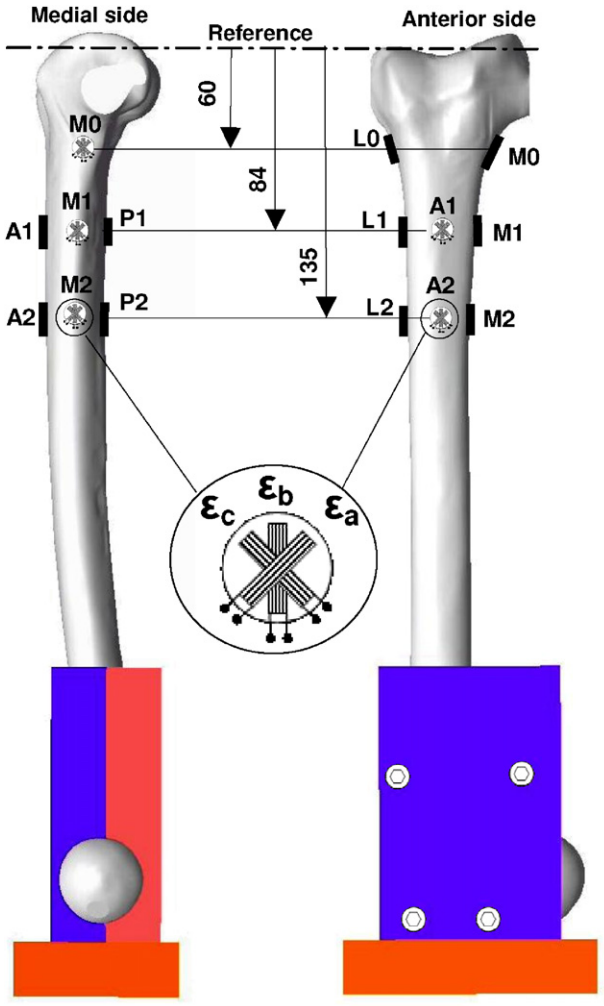

Fig. 1. Distal femur with locations of strain gauges. Bone strains were measured with 4 gauges glued at the anterior (A2 and A3) and posterior (P2 and P3) sides and 6 gauges glued at the medial (M1, M2 and M3) and lateral (L1, L2 and L3) sides of the femur.

2. Materials and methods

2.1. Experiments

Four synthetic femurs (third generation, left, model 3306, from Pacific Research Labs, Vashon Island, WA, USA) were selected and used for the experimental study. This new femur model has a cortical bone analogue consisting of short-glass-fiber-reinforced epoxy, rather than the fiber glass-fabric-reinforced epoxy of previous synthetic femur replicas. The new cortical analogue offered the possibility of improving the uniformity of mechanical properties within a synthetic bone, allowed for greater anatomic detail to be added to the bones, and simplified the fabrication process.

Triaxial (rosette) strain gauges (KFG-3-120-D17-11L3M2S, Kyowa Electronic Instruments Co., Ltd., Japan) were glued onto the medial, lateral, anterior and posterior side of the cortex at different levels proximally to the condyle surface (Fig. 1) and were used to measure surface strains. The middle strain gauge ε_b was aligned with the vertical axis of the femur. All strain gauges were connected to a data acquisition system Spider 8 (Hottinger Baldwin Messtechnik GmbH, Germany) which was connected to a PC to record the data with software Catman (Hottinger Baldwin Messtechnik GmbH, Germany). A reference axis was marked on the outer cortical surface of each synthetic femur to allow reproducible alignment and positioning of the strain gauges (Cristofolini, 1997; Ruff and Hayes, 1983). The positions of the strain gauges were also measured using a 3D coordinate measuring machine (Model Maxim, Aberlink, UK) and were used in the FE models to "pick" the strain values.

Three different femoral components of the PFC Sigma Modular Knee System (DePuy International, Inc Johnson&Johnson–Warsaw, Indiana, USA) were implanted into synthetic femurs by an experienced surgeon (Fig. 2, Table 1). The femoral components will be referred to in this paper as cemented stemless, cemented stemmed and noncemented stemmed

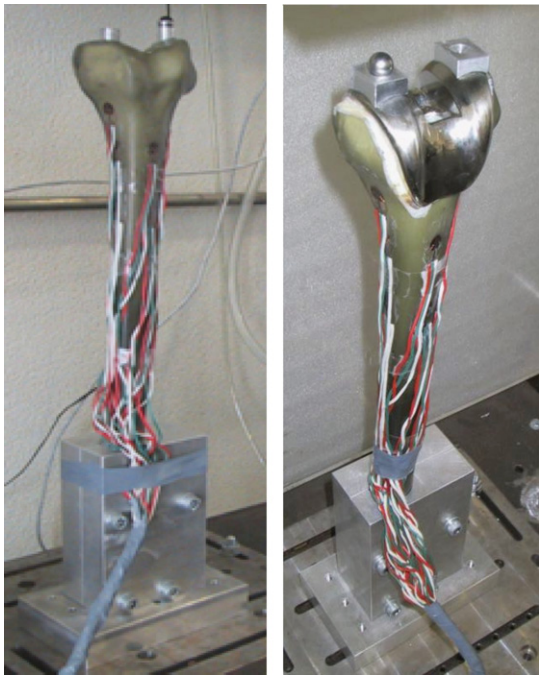

Fig. 2. Instrumented intact (left) and implanted (right) femur.

Table 1
Characteristics of the cemented stemless, cemented stemmed and noncemented stemmed distal femoral components of the PFC Sygma Modular Knee System used in the current study

Model	PFC Sigma Knee System	Stem	Cement
Stemless (a)	Size 4; Co-Cr-Mo; 71 mm ML, 65 mm AP Sacrifice of LCP		CMW 1
Cemented stem (b)	Size 4; Co-Cr-Mo; 71 mm ML, 65 mm AP, 7° Sacrifice of LCP	15 mm × 90 mm Ti-6Al-4V	CMW 1
Non-cemented stem (c)	Size 4; Co-Cr-Mo; 71 mm ML, 65 mm AP, 7° Sacrifice of LCP	18 mm × 175 mm Ti-6Al-4V	CMW 1
(a) 	(b) 	(c) 	

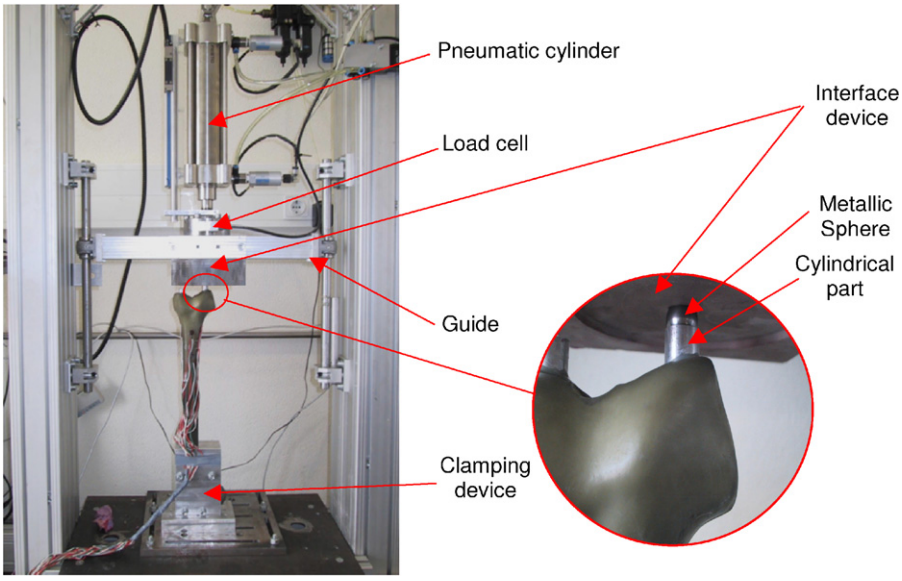

Fig. 3. Testing device. Strains were recorded for a force applied on the medial condyle (1160 N) and on the lateral condyle (870 N) separately.

components. The in vitro insertion procedure was performed according to the protocol described for this type of knee prosthesis. CMW-1 (DePuy International, Inc Johnson & Johnson–Warsaw, Indiana, USA) bone cement was used for the cemented designs and a mean thickness of 2 mm was obtained for the cement mantle. The thickness of the cement mantle was determined from AP and ML radiographs of the implanted synthetic femurs.

Bone strains were measured on all femurs under simplified loading. The femur was fixed at the great trochanter (Fig. 2) through a stiff metal device at 0° adduction. A pneumatic device was used to apply the load (vertical direction) at the medial and lateral condyles independently and at different times. As shown in Figs. 2 and 3, the load was applied directly on a metallic sphere placed on an aluminum part glued to the medial and lateral condyles. The load was controlled via a load cell (TC4 1T, AEP, Modena, Italy). Each intact and reconstructed femur replica was loaded 5 times. The loading procedure was applied according to Finlay et al. (1982) and is described in Table 2. The stabilization time E is related to the viscoelastic behavior of the synthetic femurs and is recommended by Cristofolini et al. (1996). Strains were averaged over these 5 loading repetitions. All experiments were made at room temperature ranging from 20 to 22 °C.

Table 2
Details of the test procedure utilized

Period	Desciption	Time
A	Conditioning	1 min
B	Unloading and relaxation	4 min
C	Strain gauges set to zero	15 s
D	Loading until test load at 60 N/s	[10–22 s]
E	Load stabilization	4 min
F	Data collection	1 s
G	Unloading and relaxation	4 min
H	Residual strains collected	1 s
I	Loading intervals	20 min

For each reconstruction, the force was applied separately on the medial and lateral condyles. Two different load cases were applied: load-case 1 was a vertical force of 1160 N applied at the medial condyle; load-case 2

was a vertical force of 870 N applied at lateral condyle. These loads correspond to a 3 times body weight (70 kg) distributed 40% on the lateral condyle (870 N) and 60% on the medial condyle (1160 N) of the stance phase before toeoff (Morrison, 1970).

2.2. FE analyses

To build the FE models, AP and ML radiographs were made to the in vitro reconstructions. The large left synthetic femur (model 3306, Pacific Research Labs, Vashon Island, WA, USA) was used as reference geometry for the FE analysis. It is a 3D solid model made available in public domain derived from a CT-scan dataset of a synthetic human femur replica (Cheung et al., 2004). This solid model describes the endosteal and periosteal surface of the synthetic cortex. The material properties were assigned with reference to those indicated by the manufacturer (Heiner and Brown, 2001), i.e., a synthetic cortical bone Young's modulus of 12.4 GPa and a synthetic cancellous bone Young's modulus of 0.104 GPa. A Young's moduli of 210 and 2.28 GPa (Murphy and Prendergast, 1999) were assigned for the implant (cobalt–chrome alloy) and PMMA bone cement, respectively. A Poisson's ratio of 0.3 was assigned for all materials, which were assumed to be homogeneous, isotropic and with linear elastic behavior. The boundary conditions were defined to reproduce those used in the experimental setup.

The femoral components of the knee prosthesis were digitized with a Roland LPX 250 3-D laser scanner device with a precision of 0.2 mm. Solid models of the femoral components were created with a modeling package (Catia, Dassault Systèms, France) after digitizing the surfaces. The position of each stem relative to the femur was determined from AP and ML radiographs. A solid model of the cement mantle was created for the cemented reconstruction, taking into account the size of the rasp used and cement mantle thickness measured from the radiographs. Automatic meshing of the models was done using FE meshing software HyperMesh v6.0 (Altair Engineering, Troy, Michigan, USA). The meshes were built from 4-node linear tetrahedral elements with 6 degrees of freedom (DOF)/node. These elements have no explicit shape functions: a 10 tetrahedron is generated first, then the motion of the mid-side nodes parallel to the element's edge is condensed out and the remaining perpendicular motions converted to corner rotations (Viceconti et al., 1998). This type of the element minimizes computer-processing time that depends on the contact problem between different materials with large contact surfaces like the press-fit stem. The number of elements and nodes of the meshes (Fig. 4) were chosen based on convergence tests previously performed. The meshes of the intact femur, cemented stemless, noncemented stemmed and cemented stemmed reconstructions were composed of 164,899, 168,498, 185,676 and 263,450 FEs and 36,005, 44,483, 48,127 and 60,825 nodes, respectively. For the convergence tests, the maximal displacements and maximal equivalent strains at 32 positions (medial, lateral, anterior and posterior sides) for the intact FE femur model were assessed. The convergence rate for the displacements was less than 0.2% and less than 5% for the equivalent strains for 160,000 DOF (more or less 159,000 elements and 35,000 nodes).

FE models of the stemmed reconstructions were analyzed twice, one considering the femoral stem bonded (bonded case) and the other considering the stem sliding with friction (frictional case). These models will be referred to as bonded or frictional cases. Linear analysis was performed with FEA HyperWorks software (Altair Engineering, Troy, Michigan, USA) and nonlinear analysis with MARC Research Analysis (Palo Alto, CA, USA). For the nonlinear analysis, the contact between the implant and cement/bone complex was modeled using node-to-surface algorithm. The coefficients of friction used were $\mu = 0.25$ (Stolk et al., 1998; Kleemann et al., 2002; Mann et al., 1991) for the contact between the implant and cement mantle and $\mu = 0.3$ (Shirazi-Adl et al., 1993; Rancourt et al., 1990; Viceconti et al., 2000; Fessler and Fricker, 1989) for the contact between the implant and the bone structures (cortical and cancellous). The Coulomb friction model was used.

Maximal and minimal principal FE bone strains were obtained and correspond to the experimental strain measurement sites. These strains were compared to the mean measured strains. Linear regression analyses were performed to determine the correspondence between the measured and FE strains. Within this context, linear regression analyses were performed separately for the maximal principal strains and for the

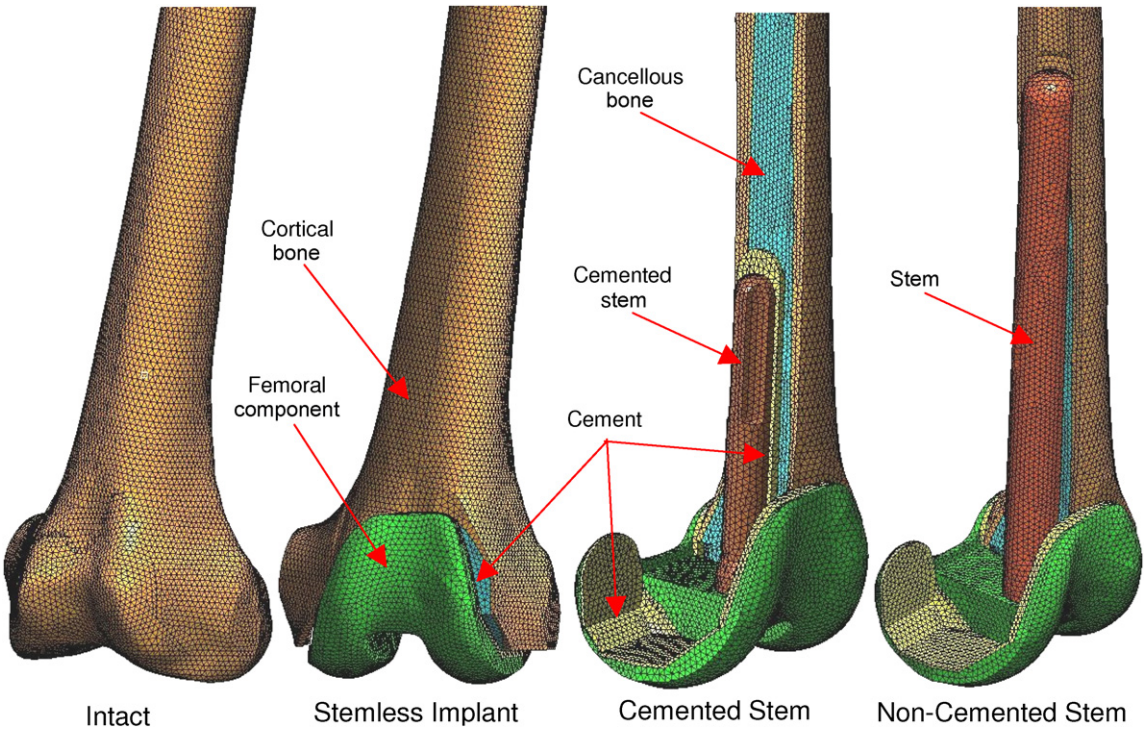

Fig. 4. FE models built and used to simulate the experiments. (a) FE model of a synthetic intact femur. (b) FE model of a synthetic reconstruction with cemented stemless implant. (c) FE model of a synthetic reconstruction with cemented stemmed implant and (d) FE model of a synthetic reconstruction with noncemented stemmed implant.

minimal principal strains. Measured strains were treated as dependent variables and FE strains as independent ones. A slope and R^2 close to 1, in combination with a small intercept, would indicate good agreement between FE and measured strains. If the intercepts were small, slopes of 0.9 and 1.1 were considered to indicate differences between experimental and FE strains of −10% and +10%, respectively. However, the intercept values must be analyzed relative to the magnitude of the strains. In fact, some differences between experimental and FE strains can be greater than 10%, which was the case for low strain values obtained with the noncemented stem simulated as bonded and with friction. An additional indicator of the overall absolute difference between FE and measured strains, the root-mean-square error (RMSE), was calculated and is defined as the square root of the average of the squared errors between FE and measured strains. The RMSE was expressed as a percentage (RMSE%) of the measured peak strain. The peak error and position is also presented.

3. Results

The FE strains and the mean experimental strains are presented in Figs. 5 and 6. A quantitative analysis using linear regressions was performed to determine the overall correspondence. The R^2, slope, interception, RMSE and peak error values are presented in Table 3. The graphs of Fig. 7 show the linear regression results for the strains in (a) intact femur model, (b) reconstruction with standard implant, (c) reconstruction with cemented stem and (d) reconstruction with noncemented stem. For the reconstruction with the noncemented stem, linear regressions were performed separately for the maximal and minimal principal strains for the bonded and friction models and are depicted in Fig. 8.

4. Discussion

Overall, comparison of the FE strains to the mean measured strains showed a close correspondence for the intact and reconstructed femurs. The standard deviation for the measured strains was smaller than 5% of the respective mean principal strain. This value was higher for mean strains less than 80 μstrain. The standard deviations are similar to those published by Heiner and Brown (2001) and Cristofolini and Viceconti (2000).

For the intact femur, the slopes of the regression lines were 0.96 for both load cases (Fig. 7(a), Table 3). The intercepts were small and the RMSE (%) values of the measured strains were less than 10% (6% and 3% for load-cases 1 and 2, respectively).

The reconstruction with the cemented stemless implant provoked FE strains similar to mean measured strains. No relevant differences were observed between FE strains from the bonded and friction cases, because no stem was present. For both bonded and friction models, the slope, interception and RMSE values were within the range of those obtained for the intact femur.

For the cemented stem, the differences between the measured and FE strains are small. Overall, the friction model produced FE strains closer to the measured ones and was more pronounced for the minimal principal strains. The slopes, interception and RMSE values were similar for both bonded and friction cases.

The highest differences between the measured and FE strains was obtained for the reconstruction femur with noncemented stem. The bone/cement–stem interface friction conditions played an important role over the maximal and minimal principal strains. The effects were more evident on the minimal principal strains. When the femur–prosthesis interface was considered bonded, the differences of minimal principal strains were pronounced. Although some differences are noticeable, most of the FE and measured maximal principal strains for the bonded case were similar. For the friction case, slopes were 1.00 and 1.03, respectively, for load-cases 1 and 2, values within the range of 0.9 and 1.1. For the bonded case, slopes were 1.61 and 1.32 for load-cases 1 and 2, respectively. Moreover, the RMSE (%) values were 15% and 14%, respectively, indicating that the objective was not achieved. In fact, no good agreement between FE and measured strains was obtained when simulating the noncemented stem as a bonded case.

Linear regressions for noncemented stem were performed for the maximal and minimal principal strains for both bonded and friction cases separately (Fig. 8). The correlation values R^2 were higher for the minimal principal strains. Low R^2 values were obtained for the maximal principal strains, 0.78 and 0.36 for the bonded and friction cases, respectively. For the minimal principal strains these were 0.95 and 0.98, respectively. The R^2 value obtained for the maximal principal strains is much lower than the same obtained considering all strains in the regression.

The cortex strains for the noncemented stem predicted by the FE models depend on the conditions assumed for the stem–cement and stem–bone interfaces. For the completely bonded interface, differences between FE and measured strains were sizeable. Within the FE models of noncemented stems we assumed a perfect contact between surfaces and therefore the degree of load transfer is higher, which is reflected on higher cortex strains. For the cemented stem, the bonded and friction FE models give strains similar to those obtained with the experimental reconstructions.

Apart from some local differences, FE and mean measured strain corresponded well for all load cases and for all intact and reconstructed femurs. Excluding the R^2 results obtained for the noncemented stem simulated as bonded, the regression analyses produced R^2 (0.92–0.99) and slopes (0.94–1.06) close to 1.0. The highest RMSE (%) value (15%) was obtained for load-case 1 for the noncemented stem simulated as bonded. For load-case 2, RMSE (%) values were 14% and 12% for the noncemented stem considered, respectively, as bonded and with friction. All other RMSE (%) values fell within the range of 10%.

It would be interesting to obtain the strains more distally, in the condyles region, but it would be technically difficult to place strain rosettes in that region of the femur

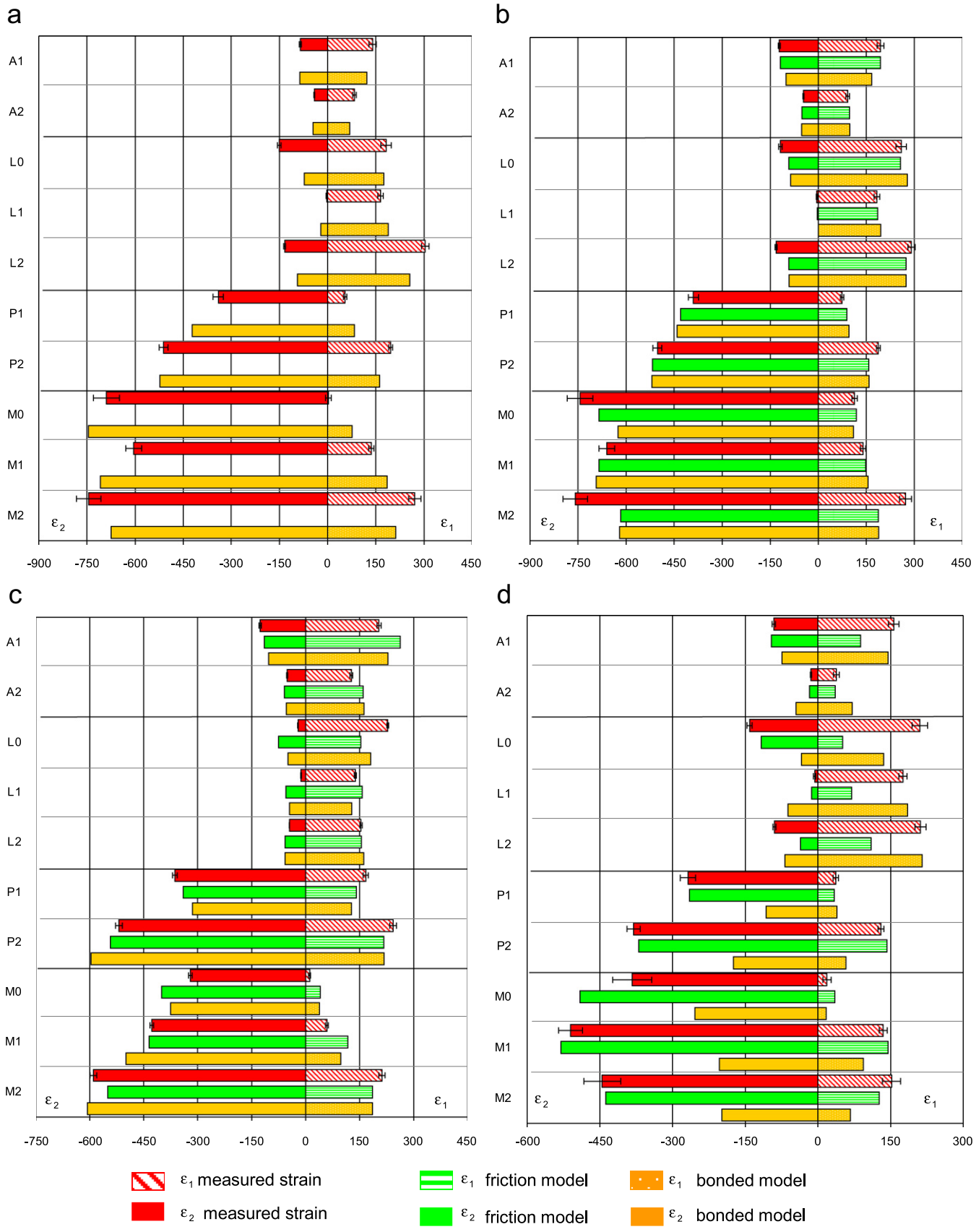

Fig. 5. Comparison of the FE and mean measured principal strains for each gauge location for a vertical force applied on the medial condyle (load-case 1). (a) Intact femur. (b) Reconstruction with cemented stemless implant. (c) Reconstruction with cemented stemmed implant and (d) reconstruction with noncemented stemmed implant. The gauge locations are named as defined in Fig. 1.

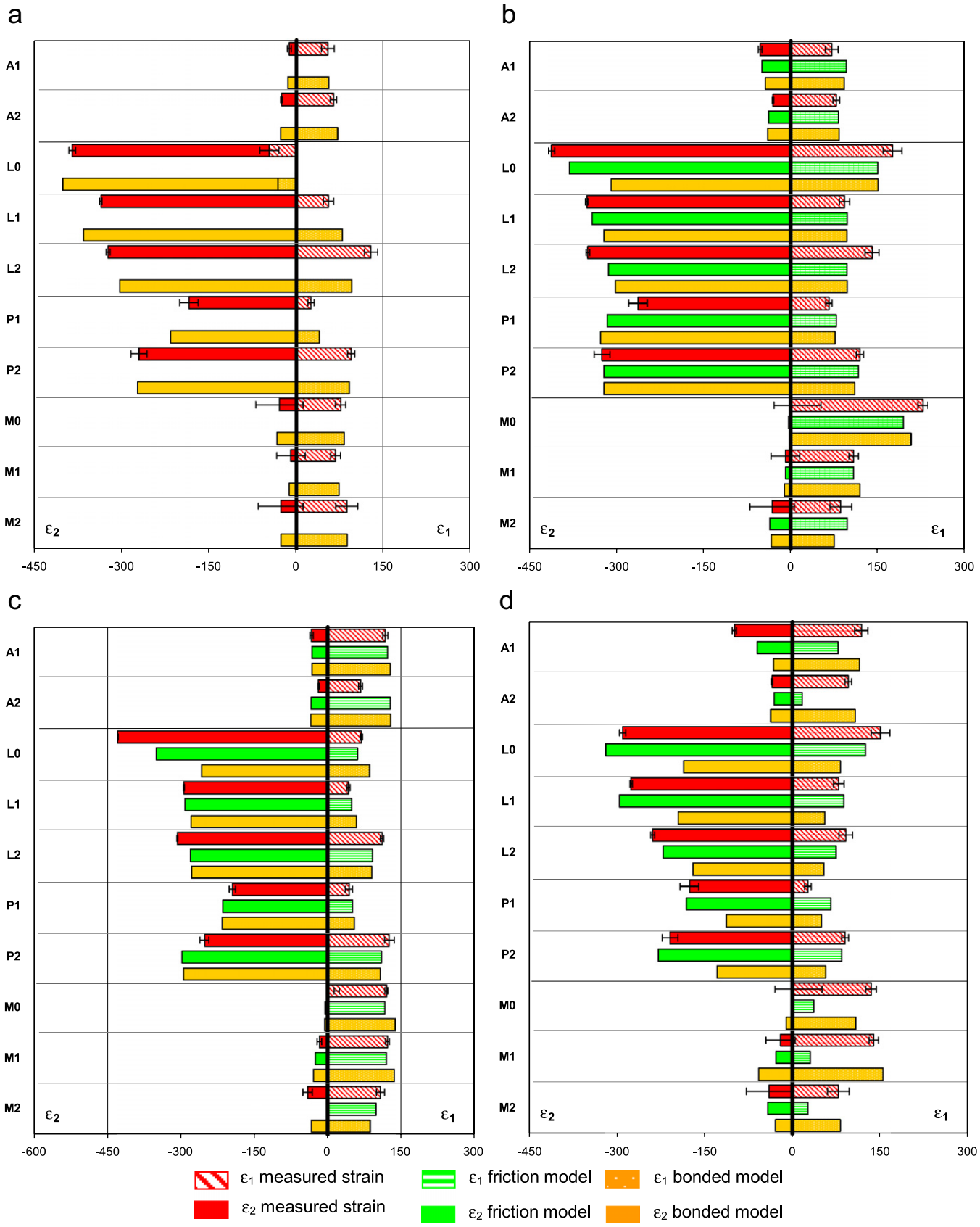

Fig. 6. Comparison of the FE and mean measured principal strains for each gauge location for a vertical force applied on the lateral condyle (load-case 2). (a) Intact femur. (b) Reconstruction with cemented stemless implant. (c) Reconstruction with cemented stemmed implant and (d) Reconstruction with noncemented stemmed implant. The gauge locations are named as defined in Fig. 1.

Table 3
Results of linear regression analysis, comparing the mean measured strains and the FE strains

Model	Interface	R^2	Slope	Intercept (mm/mm)	RMSE (mm/mm)	RMSE (%)	Peak error (position) (%)
LOAD_CASE 1							
Intact	Bonded	0.97	0.96	0.90	22	6.0	25 (M2)
Stemless	Bonded	0.98	1.06	−2.91	23	4.4	25 (M2)
	Friction	0.98	1.05	−0.26	20	3.7	25 (M2)
Cemented	Bonded	0.98	0.94	6.31	24	4.2	15 (A2)
	Friction	0.98	0.98	3.14	27	4.3	18 (A2)
Noncemented	Bonded	0.88	1.61	−27.92	72	15.0	75 (L0)
	Friction	0.94	1.00	17.82	33	7.5	76 (L0)
LOAD_CASE 2							
Intact	Bonded	0.99	0.96	0.02	9	3.0	8 (L2)
Stemless	Bonded	0.97	1.06	−0.31	21	5.1	7 (L2)
	Friction	0.98	1.02	2.52	15	3.6	21 (L2)
Cemented	Bonded	0.93	1.05	−6.34	30	6.9	38 (L1)
	Friction	0.96	1.01	−3.00	21	4.8	18 (L1)
Noncemented	Bonded	0.94	1.32	−9.12	34	14.0	46 (L0)
	Friction	0.92	1.03	16.10	30	12.0	86 (M1)

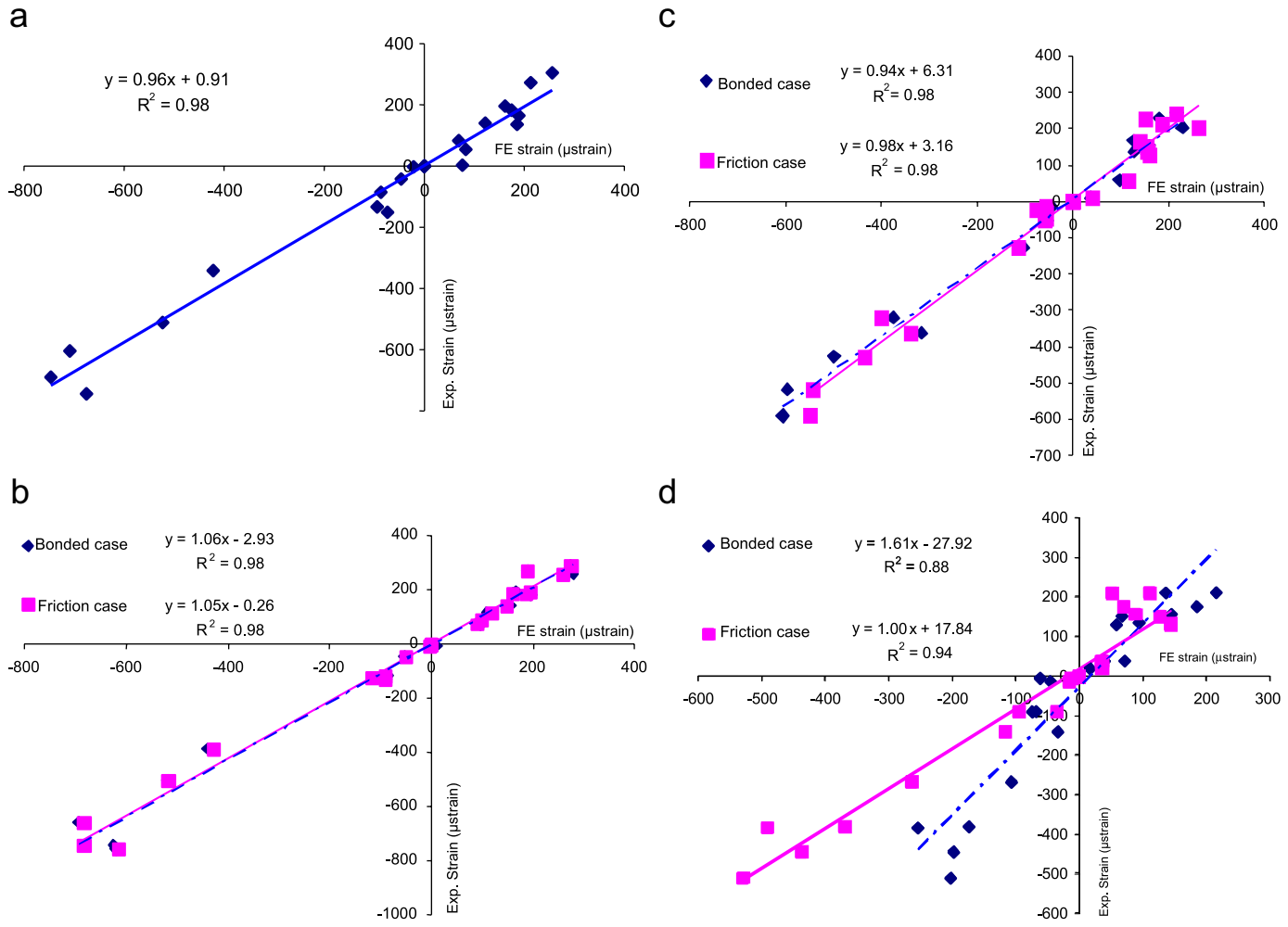

Fig. 7. Linear regression analyses were performed to determine the overall correspondence between FE and mean measured strains. The graphs show the linear regression results for the strains in (a) intact femur model, (b) reconstruction with cemented stemless implant, (c) reconstruction with cemented stemmed implant and (d) reconstruction with noncemented stemmed implant.

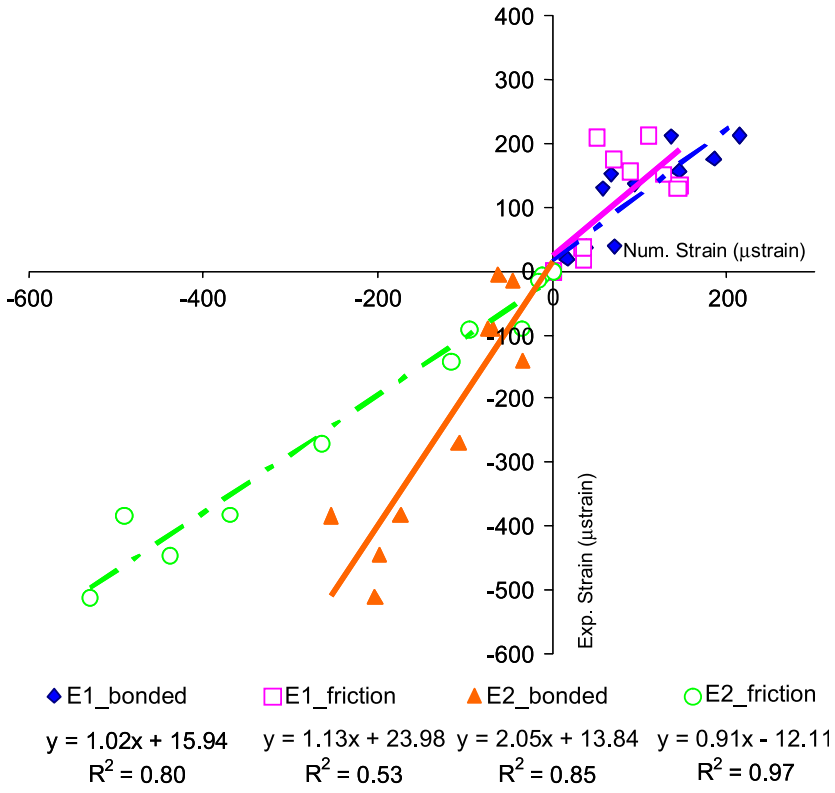

Fig. 8. Independent linear regression analyses for the minimal and maximal strains for the noncemented stem simulated as bonded and with friction (load-case 1).

without damaging them when performing the in vitro surgeries to implant the stems. However, the strains in this region of the distal femur can be assessed using the FE models, which presents, for this case, and advantage relative to the experimental models.

The study performed to validate the FE models was based on the comparison of the periosteal bone strains with different interface-bonding conditions and may be one limitation of this study. The analysis of other parameters like pre-stress, nonlinear behavior of synthetic material of cortical and cancellous bone and relative micromotion between bone and stem can also be used for a more effective FE model validation.

The FE models used in this study were successfully validated with experimental ones. This study proved that FE models of the distal femur based on modified tetrahedral elements can reproduce similar strains and was able to adequately replicate the mechanical behavior of distal femur reconstructions. Excluding the noncemented bonded stems, for both load cases, all RMSE values fall within 12%.

Aknowledgments

Fundação para a Ciência e a Tecnologia for funding António Completo through Grant SFRH/BD/18717/2004 and Johnson & Johnson for offering the knee prostheses.

References

Cheung, G., Zalzal, P., Bhandari, M., Spelt, J.K., Papini, M., 2004. Finite element analysis of a femoral retrograde intramedullary nail subject to gait loading. Medical Engineering and Physics 26, 93–108.

Cristofolini, L., 1997. A critical analysis of stress shielding evaluation of hip prostheses. Critical Reviews in Biomedical Engineering 25, 409–483.

Cristofolini, L., Viceconti, M., 1997. Comparison of uniaxial and triaxial strain gages for strain measurement in the femur. Experimental Mechanics 37 (3), 350–354.

Cristofolini, L., Viceconti, M., 2000. Mechanical validation of whole bone composite tibia models. Journal of Biomechanics 33, 279–288.

Cristofolini, L., Viceconti, M., Cappelo, A., Toni, A., 1996. Mechanical validation of whole bone composite femur models. Journal of Biomechanics 29 (4), 525–535.

Cristofolini, L., Bini, S., Toni, A., 1998. In vitro testing of a novel limb salvage prosthesis for the distal femur. Clinical Biomechanics 13, 608–615.

Crowninshield, R.D., Pedersen, D.R., Brand, R.A., 1980. A measurement of proximal femur strain with total hip artroplasty. Journal of Biomechanical Engineering 102, 230–233.

Dias Rodrigues, J.F., Lopes, H., Simões, J.A., 2004. Experimental model analysis of a synthetic composite femur. Experimental Mechanics 44 (1), 29–32.

Fessler, H., Fricker, D.C., 1989. Friction in femoral prosthesis and photoelastic model cone taper joints. Proceedings of the Institution of Mechanical Engineers Part H, Journal of Engineering in Medicine 203, 1–14.

Finlay, J.B., Bourne, R.B., McLeant, J., 1982. A technique for in vitro measurement of principal strains in the human femur. Journal of Biomechanics 15 (10), 723–739.

Grecula, M.J., Morris, R.P., Laughlin, J.C., Buford, W.L., Patterson, R.M., 2000. Femoral surface strain in intact composite femurs: a custom computer analysis of the photoelastic coating technique. IEEE Transaction on Biomedical Engineering 47, 926–933.

Heiner, A.D., Brown, T.D., 2001. Structural properties of new design of composite replicate femurs and tibias. Journal of Biomechanics 34, 773–781.

Huiskes, R., Chao, E.Y.S., 1983. A survey of finite element analysis in orthopaedic biomechanics: the first decade. Journal of Biomechanics 16, 385–409.

Huiskes, R., Weinans, H., van Rietbergen, B., 1992. The realtionship between stress shileding and bone resorption around total hip stems and the effect of flexible materials. Clinical Orthopaedics Related Research 274, 124–134.

Kleemann, R., Heller, M.O.W., Taylor, W.R., Duda, G.N., 2002. Femoral strains and cement stresses increase with anteversion and prosthesis offset in THA. In: Proceedings of the 13th Conference of the European Society of Biomechanics, Poland, p. 223.

Mann, K.A., Bartel, D.L., Wright, T.M., Ingraffe, A.R., 1991. Mechanical characteristics of the stem–cement interface. Journal of Orthopaedic Research 9, 798–808.

McNamara, B.P., Cristofolini, L., Toni, A., Taylor, D., 1994. Evaluation of experimental and finite element models of synthetic and cadaveric femora for pre-clinical design analysis. Clinical Materials 17 (3), 131–140.

Morrison, J.B., 1970. The mechanics of the knee joint in relation to normal walking. Journal of Biomechanics 3, 51.

Murphy, B.P., Prendergast, P.J., 1999. Measurement of non-linear microcrack accumulation rates in polymethylmethacrylate bone cement under cyclic loading. Journal of Materials Science 10, 779–781.

Rancourt, D., Shirazi-Adl, A., Drouin, G., Paiement, G., 1990. Friction properties of the interface between porous-surfaced metals and tibial cancellous bone. Journal of Biomedical Materials Research 24, 1503–1519.

Ruff, C.B., Hayes, W.C., 1983. Cross-section geometry of pecos pueblo femora and tibiae—a biomechanical investigation: 1. Methods and general patterns of variation. American Journal of Physical Anthropology 60, 359–381.

Shirazi-Adl, A., Dammak, M., Paiement, G., 1993. Experimental determination of friction characteristics at the trabecular bone/porous-coated metal interface in cementless implants. Journal of Biomedical Materials Research 27, 167–175.

Simões, J.A., Vaz, M.A., 2002. The Influence on strain shielding of material stiffness of press-fit femoral components. Proceedings of the Institution of Mechanical Engineers Part H Journal of Engineering in Medicine 216, 341–346.

Stolk, J., Verdonschot, N., Huiskes, R., 1998. Sensitivity of failure criteria of cemented total hip replacements to finite element mesh density. In: Proceedings of the 11th Conference of European Society of Biomechanics, Toulouse.

Stolk, J., Verdonschot, N., Cristofolini, L., Firmati, L., Toni, A., Huiskes, R., 2000. Strains in a composite hip joint reconstruction obtained through FEA and experiments correspond closely. In: Transactions of the 46th Annual Meeting of the Orthopaedic Research Society, O515.

Stolk, J., Verdonschot, N., Cristofolini, L., Toni, A., Huiskes, R., 2002. Finite element and experimental models of cemented hip joint reconstructions can produce similar bone and cement strains in pre-clinical tests. Journal of Biomechanics 35, 499–510.

Szivek, J.A., Gealer, R.L., 1991. Comparison of the deformation response of synthetic and cadaveric femora during simulated one-legged stance. Journal of Applied Biomaterials 2 (4), 277–280.

Szivek, J.A., Thomas, M., Benjamim, J.B., 1993. Characterisation reponse of synthetic and cadaveric femora during simulated one-legged stance. Journal of Applied Biomaterials 2, 277–280.

Verma, A., Melosh, R.J., 1987. Numerical tests for assessing finite element model convergence. International Journal for Numerical Methods in Engineering 24, 843–857.

Viceconti, M., Casali, M., Massari, B., Cristofolini, L., Bassini, S., Toni, A., 1996. The 'Standardized femur program'. Proposal for a reference geometry to be used for the creation of finite element models of the femur. Journal of Biomechanics 29, 1241.

Viceconti, M., Bellingeri, L., Cristofolini, L., Toni, A., 1998. A comparative study on different methods of automatic mesh generation of human femurs. Medical Engineering and Physics 20, 1–10.

Viceconti, M., Muccini, R., Bernakiewicz, M., Baleani, M., Cristofolini, L., 2000. Large-sliding contact elements accurately predict levels of bone-implant micromotion relevant to osseointegration. Journal of Biomechanics 33, 1611–1618.

Young-Hoo, K., Kim, J.S., Cho, S.H., 2001. Strain distribution in the proximal human femur. Journal of Bone and Joint Surgery 83, 295–301.